Mitochondrial SOD2 regulates epithelial-mesenchymal transition and cell populations defined by differential CD44 expression

Hideaki Kinugasa[1,2,3,*], **Kelly A. Whelan**[1,2,*], **Koji Tanaka**[1,2], **Mitsuteru Natsuizaka**[1,2,4], **Apple Long**[1,2], **Andy Guo**[1,2], **Sanders Chang**[1,2], **Shingo Kagawa**[1,2], **Satish Srinivasan**[5], **Manti Guha**[5], **Kazuhide Yamamoto**[3], **Daret K. St. Clair**[6], **Narayan G. Avadhani**[5], **J. Alan Diehl**[2,7], and **Hiroshi Nakagawa**[1,2]

[1]Gastroenterology Division, Department of Medicine, University of Pennsylvania, Philadelphia, Pennsylvania

[2]Abramson Cancer Center, University of Pennsylvania, Philadelphia, Pennsylvania

[3]Department of Gastroenterology and Hepatology, Okayama University Graduate School of Medicine, Dentistry, and Pharmaceutical Sciences, Okayama, Japan

[4]Department of Gastroenterology and Hepatology, Hokkaido University, Sapporo, Japan

[5]Department of Animal Biology, Mari Lowe Center for Comparative Oncology, School of Veterinary Medicine, University of Pennsylvania, Philadelphia, Pennsylvania

[6]Graduate Center for Toxicology, University of Kentucky College of Medicine, Lexington, Kentucky

[7]Department of Biochemistry and Molecular Biology, Medical University of South Carolina, Charleston, South Carolina

Abstract

Epithelial-mesenchymal transition (EMT) promotes cancer cell invasion, metastasis and treatment failure. EMT may be activated in cancer cells by reactive oxygen species (ROS). EMT may promote conversion of a subset of cancer cells from a CD44^{Low}-CD24^{High} (CD44L) epithelial phenotype to a CD44^{High}-CD24$^{-/Low}$ (CD44H) mesenchymal phenotype, the latter associated with increased malignant properties of cancer cells. ROS are required for cells undergoing EMT while excessive ROS may induce cell death or senescence; however, little is known as to how cellular antioxidant capabilities may be regulated during EMT. Mitochondrial superoxide dismutase 2 (SOD2) is frequently overexpressed in oral and esophageal cancers. Here, we investigate mechanisms of SOD2 transcriptional regulation in EMT as well as the functional role of this antioxidant in EMT. Using well-characterized genetically engineered oral and esophageal human epithelial cell lines coupled with RNA interference (RNAi) and flow cytometric approaches, we find that transforming growth factor (TGF)-β stimulates EMT, resulting in conversion of CD44L

Correspondence: Hiroshi Nakagawa, M.D., Ph.D., 956 BRB, Gastroenterology Division, University of Pennsylvania, 421Curie Blvd., Philadelphia, PA 19104- 4863, USA, Telephone: 215-573-1867, FAX: 215-573-2024, nakagawh@mail.med.upenn.edu.
*KA Whelan and H Kinugasa contributed equally to this work.

to CD44H cells, the latter of which display SOD2 upregulation. SOD2 induction in transformed keratinocytes was concurrent with suppression of TGF-β-mediated induction of both ROS and senescence. SOD2 gene expression appeared to be transcriptionally regulated by NF-κB and ZEB2, but not ZEB1. Moreover, SOD2-mediated antioxidant activity may restrict conversion of CD44L cells to CD44H cells at the early stages of EMT. This data provides novel mechanistic insights into the dynamic expression of SOD2 during EMT. Additionally, we delineate a functional role for SOD2 in EMT via the influence of this antioxidant upon distinct CD44L and CD44H subsets of cancer cells that have been implicated in oral and esophageal tumor biology.

Keywords

SOD2; MnSOD; epithelial-mesenchymal transition; esophageal squamous cell carcinoma; reactive oxygen species; CD44

Introduction

Epithelial-mesenchymal transition (EMT) is a developmental process whereby epithelial cells lose their defining features (e.g. cell-cell adhesion and polarity) to gain mesenchymal characteristics including increased motility and fibroblastic spindle-shaped morphology [1, 2]. EMT has been implicated in the pathogenesis of variety of diseases, both benign and malignant [1, 2]. EMT contributes to cancer cell invasion, metastasis and treatment failure [3, 4] and may be activated via reactive oxygen species (ROS) generated in response to stimuli in the tumor microenvironment (e.g. hypoxia and inflammatory cytokines) and therapeutic agents [5]. Furthermore, oncogene activation promotes ROS accumulation [6]. During the early stages of carcinogenesis, oncogene-induced ROS may promote EMT in premalignant epithelial cells to negate oncogene-induced senescence, serving as a fail-safe mechanism to prevent malignant transformation [7].

Malignant properties of cancer cells have been linked to cell surface expression of CD44, a major receptor for hyaluronic acid, which mediates crosstalk between cancer cells and the surrounding microenvironment [8]. A high level of CD44 is also associated with self-renewal and tumor initiating capabilities in subsets of cancer cells referred to as cancer stem cells (CSCs) [8-10]. A variety of cell surface markers including CD24 have been used in conjunction with CD44 to identify CSCs. Specifically, CD24/CD44 expression pattern exhibits a robust shift during EMT, as $CD44^{Low}$-$CD24^{High}$ (CD44L) epithelial cells are converted to $CD44^{High}$-$CD24^{-/Low}$ (CD44H) mesenchymal cells. Moreover, acquisition of characteristics of stemness has been shown to accompany EMT-mediated CD44L-to-CD44H cell conversion [11, 12].

Little is known as to how ROS are regulated during EMT or the induction of CD44H cells. Although excessive ROS cause cellular oxidative stress, ROS are also essential in physiological processes including cell signaling, proliferation, differentiation and metabolic adaptation [13, 14]. A major cellular source of ROS is mitochondria, where highly reactive superoxide (O_2^-) is produced as a byproduct of respiration [15]. As a potent inducer of EMT, transforming growth factor (TGF)-β stimulates ROS, but also requires the production of mitochondrial superoxide for EMT [16, 17]. However, senescence, in addition to EMT, may

occur in response to TGF-β in human epithelial cells [18]. Mitochondrial ROS have a role in TGF-β-mediated senescence [19]. Differential cell fates induced by TGF-β may be in part accounted for by genetic alterations associated with malignant transformation, which enrich EMT-competent cells [20]. Moreover, EMT may be influenced by cellular antioxidant capability which may limit ROS to a level that is permissible for EMT, but not senescence or cell death.

Superoxide radicals in mitochondria are removed by the mitochondrial enzyme superoxide dismutase 2 (SOD2 aka MnSOD), generating hydrogen peroxide (H_2O_2) and molecular oxygen. H_2O_2 is then further detoxified by catalase, glutathione peroxidase or peroxiredoxins [21]. SOD2 is an 88-kDa protein, encoded by a gene on chromosome 6q25 [22, 23]. Many proinflammatory cytokines, growth factors and redox active agents induce SOD2 expression through transcriptional, posttranscriptional and posttranslational regulatory mechanisms [22, 23]. Amongst transcription factors well-characterized in the regulation of SOD2 expression are Sp1 and NF-κB. Sp1 maintains the basal promoter activity of SOD2 while NF-κB enhances SOD2 transcription mainly via a *cis*-element within the second intronic enhancer region [23]. SOD2 is often overexpressed in aggressive cancers and has been linked to the enhancement of tumor cell migration and invasion [24]. Although NF-κB has been implicated in TGF-β-mediated EMT [25], it remains unclear as to how NF-κB may regulate EMT. Moreover, many genes (e.g. E-cadherin and N-cadherin) are concurrently regulated by multiple EMT-inducing transcription factors [26] including zinc finger E-box binding proteins ZEB1 and ZEB2. While ZEB1 and ZEB2 are both essential in TGF-β-mediated EMT [27]; their role in SOD2 expression has yet to be elucidated.

In this study, we explored the transcriptional regulation and functional role of SOD2 in well-defined transformed oral and esophageal human epithelial cell lines undergoing EMT. We find that NF-κB and ZEB2 contribute to SOD2 gene expression in CD44H cells and that SOD2-mediated antioxidant activity influences the induction of CD44H cells via EMT.

Results

SOD2 is induced during EMT-mediated conversion of CD44L to CD44H cells

We suspected that cellular antioxidants may be induced to limit oxidative stress during EMT. We previously reported that TGF-β induces EMT robustly in transformed esophageal epithelial cells compared to non-transformed cells [20]. Indeed, both EPC2-hTERT-EGFR-p53^{R175H} (transformed) and EPC2-hTERT-neo-puro (non-transformed) cells exhibited acquisition of spindle-shaped morphology and E-cadherin-N-cadherin switching in response to TGF-β, albeit with a more pronounced response occurring in transformed EPC2-hTERT-EGFR-p53^{R175H} cells (Fig. 1 A-C). To further characterize EMT, we analyzed expression of the cell surface markers CD24 (induced upon squamous cell differentiation) and CD44 (receptor for hyaluronic acid) as EMT has been shown to induce a shift in the expression of these two antigens, with epithelial cells exhibiting a CD44^{Low}-CD24^{High} (CD44L) expression profile that moves toward a CD44^{High}-CD24$^{-/Low}$ (CD44H) distribution in mesenchymal cells[11, 12]. Using flow cytometry, we found that both EPC2-hTERT-neo-puro and EPC2-hTERT-EGFR-p53^{R175H} cells encompass discrete CD44L and CD44H populations (Figure 1D). EMT induction in both cell lines was mirrored by conversion of

CD44L cells to CD44H cells (Fig. 1D and E); however, this conversion was more apparent in EPC2-hTERT-EGFR-p53^{R175H} cells, consistent with enhanced EMT in response to TGF-β as compared to EPC2-hTERT-neo-puro cells. Moreover, as EPC2-hTERT-EGFR-p53^{R175H} cells were less susceptible to ROS and senescence upon TGF-β stimulation in comparison to EPC2-hTERT-neo-puro cells (Fig. 1F and G), we suspected that cellular antioxidants may be induced to limit oxidative stress during EMT in transformed keratinocytes. Indeed, examination of antioxidant protein expression revealed induction of SOD2, catalase and GPX during EMT in transformed EPC2-hTERT-EGFR-p53^{R175H}, with mitochondrial SOD2 exhibiting the most robust upregulation (Fig. 1B and C).

We next employed FACS to isolate CD44L and CD44H cells and determine whether these subpopulations display differential SOD2 expression. When isolated from EPC2-hTERT-EGFR-p53^{R175H}, CD44L and CD44H cells repopulated within 1-2 weeks in subsequent culture, precluding their separate propagation for further functional analyses (Supplemental Figure S1). By contrast, CD44L and CD44H cells isolated from EPC2T, a derivative of EPC2-hTERT-EGFR-p53^{R175H} with cyclin D1 overexpression, did not repopulate as rapidly, permitting further analyses of separate CD44L and CD44H populations (Supplemental Figure S1). Examination of E-cadherin and N-cadherin expression patterns validated the epithelial and mesenchymal characteristics of EPC2T CD44L and CD44H cells, respectively (Figure 2A). Moreover, in addition to upregulation of the EMT-associated transcription factors ZEB1 and ZEB2, EPC2T CD44H cells showed significantly elevated expression of SOD2 as well as GPX1 and catalase (Fig. 2A and B). CD44H cells specifically displayed increased expression of the 1.5-kb transcriptional variant of SOD2 that has been associated with quiescent cells [28] with no significant change in expression of 4.2-kb transcript (Figure 2B). Immunofluorescent staining further confirmed that SOD2 expression was enhanced in CD44H EPC2T cells compared their CD44L counterparts (Figure 2C). Furthermore, CD44H cells purified from the genetically engineered oral keratinocyte cell line OKF6-hTERT-EGFR-p53^{R175H} exhibited SOD2 upregulation although they repopulated faster than that of those from EPC2T as corroborated by N-cadherin expression detected in CD44L and E-cadherin expression detected in CD44H populations (Figure 2D; Supplemental Figure S1). Taken together, these data suggest that SOD2 induction may be associated with the conversion of CD44L cells to CD44H cells via EMT.

NF-κB and ZEB2 contribute to transcriptional induction of SOD2 in CD44H cells

We next aimed to investigate mechanisms regulating SOD2 induction in EMT cells. Gene array analysis comparing CD44L and CD44H cells from EPC2-T revealed significant upregulation of multiple NF-κB target genes (e.g. IL6 and IL8) in CD44H cells (GSE37993). Based upon these findings, which were validated by quantitative RT-PCR (Figure 3A) and previous reports identifying a role for NF-κB in the regulation of SOD2 expression [23, 29], we hypothesized that NF-κB may regulate SOD2 induction during EMT. Activation of NF-κB in EPC2T CD44H cells was corroborated by increased NF-κB p65^{Ser536} phosphorylation level and basal NF-κB reporter activity (Fig. 3B and C). To test the involvement of NF-κB in SOD2 expression, we performed NF-κB knock down by RNAi directed against NF-κB p65. This resulted in suppression of the NF-κB reporter activity

(data not shown) as well as the expression of NF-κB p65, IL6, IL8 and SOD2 (Fig. 3D and E). Of note, NF-κB knockdown did not affect the expression of E-cadherin and N-cadherin in CD44L and CD44H cells (data not shown). We further tested the transcriptional activities of SOD2 in CD44L and CD44H cells with well-characterized SOD2 promoter reporter constructs [29-31]. P7/pGL3 and I2E-P7/pGL3 contain the basal SOD2 promoter (-210 to +24) with the latter carrying a major NF-κB binding *cis*-element within the SOD2 second intron enhancer (I2E) region. pSODLUC-3340 contains the 3.3-kb SOD2 5′-flanking region. Of note, basal transcriptional activity of the pSODLUC-3340 reporter in CD44L cells was markedly lower than that of either P7/pGL3 or I2E-P7/pGL3, perhaps due to the presence of a negative regulatory element in this 3.3-kb construct. Nevertheless, I2E-P7/pGL3 showed significantly elevated reporter activity in CD44H cells as compared to CD44L cells, suggesting a role for the NF-κB *cis*-element in SOD2 upregulation in CD44H cells (Figure 3F). NF-κB binding was suggested by decreased I2E-P7/pGL3 reporter activity upon introduction of RNAi directed against NF-κB (Figure 3F). Moreover, NF-κB knockdown reduced pSODLUC-3340 and P7/pGL3 reporter activities in CD44H, but not CD44L cells (Figure 3F), indicating that the NF-κB may also indirectly influence SOD2 transcription activity in CD44H cells. A similar effect was observed when NF-κB was pharmacologically suppressed by IKK-2 Inhibitor IV (data not shown).

In addition to NF-κB, ZEB1 and ZEB2 were upregulated in CD44H cells (Figure 2A; Supplemental Figure S2) amongst transcription factors essential in EMT in transformed human esophageal cell lines including EPC2-hTERT-EGFR-p53^{R175H} and EPC2T [20, 32]. We next questioned whether ZEB1 and ZEB2 may be regulated by NF-κB to influence *SOD2* transcription. NF-κB knockdown did not affect ZEB1 or ZEB2 expression (Figure 3E), suggesting that ZEBs are not directly regulated by NF-κB in CD44H cells. Interestingly, however, knockdown of ZEB2, but not ZEB1, resulted in attenuation of SOD2 expression in EPC2T CD44H cells (Fig. 4A and B). Moreover, ZEB2 knockdown repressed all SOD2 reporters including P7/pGL3 lacking an NF-κB binding *cis*-element (Figure 4C), suggesting that ZEB2 influences basal SOD2 promoter activity, although *in silico* analysis by the ECR browser [33] did not identify a conserved ZEB-binding box within the proximal SOD2 regulatory region (data not shown). These results suggest that SOD2 may be subjected to direct and indirect regulation via multiple transcription factors including NF-κB and ZEB2 during EMT.

The antioxidant activity of SOD2 restricts conversion of CD44L cells to CD44H cells

We next evaluated the antioxidant capabilities of CD44L and CD44H subpopulations isolated from EPC2T and OKF6-hTERT-EGFR-p53^{R175H} cell lines in response to hypoxia or H_2O_2. In both cell lines, ROS induction in response to these oxidative stress-inducing stimuli was limited in CD44H cells as compared to CD44L cells (Fig. 5A and B), in agreement with increased expression of antioxidants in CD44H cells (Figure 2; data not shown). To clarify the functional involvement of SOD2, we utilized RNAi to suppress SOD2 expression in EPC2T CD44L and CD44H cells (Figure 5C). SOD2 knockdown raised basal ROS level significantly in CD44L cells (Fig. 5D and E), suggesting diminished antioxidant capability as a result of SOD2 knockdown. The RNAi effect in CD44H cells, however, appeared to be modest, with limited impact upon ROS (Fig. 5D and E), likely due

to higher basal SOD2 expression (Figure 5C). Moreover, SOD2 knockdown made EPC2T CD44L cells prone to ROS induction upon exposure to H_2O_2, hypoxia or TGF-β (Figure 5E), indicating that cells expressing lower SOD2 may be more susceptible to oxidative stress. In agreement, SOD2 knockdown did not allow CD44H cells to produce as much ROS as were observed in CD44L cells upon H_2O_2, hypoxia or TGF-β stimulation (Figure 5E). Of note, we found that treatment with the antioxidant compound N-acetylcysteine (NAC) was sufficient to suppress basal ROS in EPC2T cells, thereby confirming the specificity of DCF as metric for ROS (Supplemental Figure S3A). Additionally, NAC significantly suppressed TGF-β-mediated CD44H expansion in EPC2T cells (Supplemental Figure S3B), consistent with reports indicating that ROS are critical mediators of EMT [16, 34].

We next sought to investigate the role of SOD2 in the conversion of CD44L cells to CD44H cells. We first asked how SOD2 knockdown may alter the cell distribution within EPC2T where CD44L cells represent the majority of cells. When SOD2 was knocked down by transient transfection, the percentage of CD44H cells was increased within 4 days after siRNA was transfected into the cells (Fig. 6A and B). This was further confirmed with purified CD44L cells. When CD44L cells (>99.8% purity) were transfected with siRNA directed against SOD2 and stimulated with TGF-β, CD44H cells were induced more efficiently than control cells treated with either SOD2 knockdown alone or TGF-β stimulation alone (Figure 6C). Based upon these findings along with studies indicating that mitochondrial superoxide is induced at the onset of EMT [16, 17], we suspected that SOD2 may suppress intracellular ROS level to limit the ability of CD44L cells to undergo EMT in response to stimuli causing oxidative stress. Indeed, purified CD44L cells stimulated with TGF-β, display a 40-50% decrease in SOD2 RNA expression in the first 6 days of treatment (Figure 6D). Interestingly, SOD2 expression then increased gradually again after 14 days of TGF-β treatment with a robust induction at days 21 and 25, potentially due the accumulation of CD44H cells at these later time points (Figure 6D). Further characterization of ROS in EPC2T subpopulations revealed that ROS level is highest in a minor population of cells that can be found between the CD44L and CD44H populations (Figure 6E), suggesting that induction of ROS may be critical for EMT-mediated CD44L to CD44H cell conversion. These "transitioning" cells, designated CD44T, which are induced along with CD44H cells in response to SOD2 knockdown in EPC2T cells (Supplemental Figure S4), have the potential to provide further insight into the dynamic role of SOD2 in EMT and cell fate decisions in response to environmental cues.

Taken together our findings suggest that SOD2 is subjected to dynamic regulation to exert a critical antioxidant function, which may control EMT and generation of CD44H cells. SOD2 expression may first be downregulated in CD44L cells to augmented ROS production, facilitating EMT-mediated CD44H cell expansion; however, once CD44L cells have converted to CD44H cells, ZEB2 may raise SOD2 expression along with NF-κB, increasing cellular antioxidant capability.

Discussion

In this study, we have demonstrated that SOD2 is induced in cells undergoing EMT and that SOD2 is upregulated in CD44H cells with mesenchymal characteristics (Fig. 1 and 2). NF-

κB activity was increased to stimulate SOD2 transcription in CD44H cells (Figure 3), where ZEB2 also increased basal SOD2 promoter activity (Figure 4). Finally, SOD2 knockdown experiments suggested that the low level of SOD2 expressed in CD44L cells may prevent ROS from being elevated to facilitate EMT to allow conversion to CD44L cells to CD44H cells (Fig. 5 and 6).

Antioxidant activities in CD44H cells have been implicated in EMT and cancer stem cells from squamous cell carcinomas of the head and neck [35, 36] and esophageal [37] epithelial cells, which are relevant to the cell lines we used in this study. Our data demonstrates that multiple antioxidants are induced during EMT and in CD44H cells (Fig. 1 and 2). Glutathione may be upregulated in the reduced state to exert antioxidant activities in cancer stem cells expressing variant isoforms of CD44 [38]; however, to date no functional relationship has been established between SOD2 and CD44 despite their potential roles in the redox regulation and malignant properties of cancer cells. SOD2 may have a role in tumor cell migration and invasion [24] although SOD2 expression and activity can be either increased or decreased in cancers [23]. To our knowledge, this is the first functional study exploring the role of SOD2 induction in EMT. One significant implication is that SOD2 expression may be robustly altered during EMT within a genetically engineered single cell line carrying known genetic alterations (e.g. EGFR overexpression and p53 mutation). Thus, variable SOD2 expression in cancer cells may be accounted for by not only genetic changes (e.g. loss of functional p53 [39]) gained at different disease stages but intratumoral cancer cell heterogeneity associated with EMT as documented in esophageal squamous cell carcinoma [32]. Given mitochondrial localization of SOD2, our study also reinforces the emerging roles of mitochondria in regulation of EMT and cancer stem cells [40].

Regulation of SOD2 expression has been extensively studied at both transcriptional and post-transcriptional levels [23]. Our findings (Figure 3) reinforce the crucial role of NF-κB in regulating SOD2 transcription. In addition, NF-κB may have a unique role in EMT by regulating SOD2, but not necessarily common EMT markers such as E-cadherin and N-cadherin. Both ZEB1 and ZEB2 regulate these cadherin molecules in EPC2-hTERT derivatives including EPC2T used in this study [20, 32] and NF-κB induces ZEB1 and ZEB2 in mammary epithelial MCF10A cells undergoing EMT [41]. NF-κB knockdown, however, affected neither ZEB1 nor ZEB2 in EPC2T (Figure 3E), implying a cell-type specific role of NF-κB that is independent of regulation of cadherin expression. SOD2 transcription and mRNA expression were suppressed by RNAi directed against either NF-κB or ZEB2, but not ZEB1 (Fig. 3 and 4). Interestingly, NF-κB knockdown suppressed P7/pGL3 reporter activity sharply in CD44H cells although this construct lacks a known NF-κB binding site unlike the I2E-P7/pGL3 construct, suggesting that CD44H cells may have not only a higher NF-kB activity but an increased dependence upon NF-κB for SOD2 expression. Moreover, ZEB2 knockdown had a similar impact upon all constructs (Figure 4C), indicating that ZEB2 may target common *cis*-elements within the proximal GC-rich basal promoter region (-210 to +24) shared by all constructs even though there is no consensus ZEB binding site within this region. Given the role of Sp1 in basal SOD2 transcription activation [31], our data agree with a model proposed by Dhar and St. Clair, [23] where a common factor(s) (e.g. nucleophosmin) may bridge multiple transcription factors (i.e. Sp1 and NF-κB) binding

separate *cis*-elements to regulate SOD2 transcription. Interestingly enough, ZEB2 has been recently shown to stabilize and upregulate Sp1 to induce mesenchymal cadherin-11 as well as integrin α5 during EMT to promote cancer cell invasion [42, 43]. While NF-κB may induce SOD2, SOD2 may activate NF-κB to promote EMT by stimulating IKKβ transcription in lung adenocarcinoma cells [44], suggesting a positive feedback mechanism for SOD2 expression during EMT.

At post-transcriptional levels, several microRNAs (miR-146a, miR-212, miR-222, miR-335, miR-377 and miR-382) have been shown to target SOD2 [45-50]. Interestingly, miR-382 was found to suppress SOD2 to promote TGF-β-mediated EMT in renal epithelial cells [48]. By contrast, miR-212 suppressed SOD2 to prevent EMT in colorectal cancer cells [45]. In CD44L cells, TGF-β decreased SOD2 mRNA expression earlier (Figure 6D) prior to the transition of E-cadherin-to-N-cadherin during EMT. This suggests that SOD2 expression may be subjected to a biphasic regulation during EMT. Given the requirement of mitochondrial superoxide at the onset of EMT [16, 17], a transient suppression of SOD2 may permit TGF-β-induced ROS to reach a level that triggers the conversion of CD44L cells to CD44H cells. Of two known SOD2 transcripts [28], our data (Figure 2B) indicated that the short 1.5-kb transcriptional variant is a dominant form of SOD2 mRNA expressed especially in CD44H cells compared with the 4.2-kb transcript which has a long 3′-untranslated region containing multiple potential microRNA binding sites. Thus, SOD2 upregulation in CD44H cells may be accounted for by the lack of microRNA-mediated negative regulation through the 4.2-kb transcript. Since the 1.5-kb SOD2 transcript is expressed in quiescent cells[28], this is also consistent with the upregulation of 1.5-kb transcript (Figure 2B) in less proliferative mesenchymal CD44H cells.

An earlier study showed that SOD2 may inhibit EMT in mammary epithelial cells by suppressing mitochondrial ROS [16]. As such, the roles of SOD2 in EMT may be complex and context-dependent. Indeed, cells may fail to undergo EMT in the presence of excessive ROS as observed in non-transformed EPC2-hTERT-neo-puro cells (Fig. 1F and G). Besides EMT, ZEB1 and ZEB2 are essential for cells to negate senescence in response to TGF-β stimulation [20] where both ZEBs repress the expression of cyclin-dependent kinase inhibitor p16^{INK4A}, essential in cell-cycle arrest associated with senescence. Thus, ZEB2 may prevent excessive ROS from inducing senescence via SOD2. In line with the above discussed premise about SOD2 repression at the early phase of EMT, our SOD2 knockdown experiments suggested that SOD2 may have a critical antioxidant role to limit EMT in CD44L cells (Figure 6); however, our data provided limited information due to the transient nature of siRNA transfection and suboptimal transfection and/or RNAi efficiency in CD44H cells. Thus, future experiments will require utilization of a system allowing complete loss of SOD2 expression to delineate better the functional roles of SOD2 in EMT, generation and maintenance of CD44H cells both *in vitro* and *in vivo*.

In addition to providing insight into the functional role of SOD2 in EMT, this study offers EPC2T cells as a tool for investigation of the dynamics underlying EMT. Interestingly, CD44L and CD44H subpopulations isolated from EPC2T (i.e. EPC2-hTERT-EGFR-p53^{R175H}-cyclinD1) display limited spontaneous CD44L-to-CD44H and CD44H-to-CD44L conversion as compared to EPC2-hTERT-EGFR-p53^{R175H} and OKF6-hTERT-EGFR-

p53[R175H] (Supplemental Figure S1), suggesting a potential negative role for cyclin D1 in facilitating keratinocyte plasticity. Despite well-established oncogenic functions, the role of cyclin D1 as it relates to EMT and cancer stem cells remains unclear. For instance, a recent study in prostate cancer reports that cyclin D1 signaling anti-correlates with EMT-associated gene expression while also driving the expansion of an existing prostate stem cell pool [51]. Evaluation of characteristics associated with stemness and tumorigenicity in CD44L and CD44H subpopulations isolated from EPC2-hTERT-EGFR-p53[R175H] cells with and without ectopic cyclin D1 expression are ongoing and have the potential to provide further insight into the role of cyclin D1 in epithelial cell fate decisions. Furthermore, the differential repopulation abilities of genetically engineered transformed esophageal keratinocytes in presence or absence of ectopic cyclin D1 expression provide a tractable system for monitoring both EMT and the reverse process of mesenchymal-epithelial transition (MET).

Materials and Methods

Cell culture, treatment and morphological assessment

EPC2-hTERT (telomerase-immortalized normal human esophageal keratinocytes), OKF6-TERT-2 (telomerase-immortalized normal human oral keratinocytes) and transformed derivatives (EPC2-hTERT-neo-puro, EPC2-hTERT-EGFR-p53[R175H], EPC2T and OKF6-hTERT-EGFR-p53[R175H]) were established and grown in keratinocyte-serum free medium (Life Technologies, Carlsbad, CA) at 37°C in a 5% CO_2 atmosphere as described previously [20, 52]. Countess™ Automated Cell Counter (Life Technologies) was used to count cells with 0.2% Trypan Blue dye to exclude dead cells. Cells were treated with 5 ng/ml of recombinant human TGF-β1 (R&D Systems, Minneapolis, MN) reconstituted in 4 mM HCl containing 0.1% bovine serum albumin. A cell-permeable IKK-2 Inhibitor IV (Cat. No. 401481, EMD Millipore, Billerica, MA) was supplied in dimethyl sulfoxide (vehicle) and used to inhibit NF-κB activity at 20 nM. Phase contrast images were acquired using a Nikon Eclipse TS100 microscope. Spindle-shaped cells were scored by counting at least 100 cells per high-power field (n=6) under light microscopy. Senescence-associated β-Galactosidase expressing cells were scored by counting at least 100 cells high-power field (n=6) under light microscopy as described [18, 20].

RNA interference (RNAi) and transfection

Small interfering RNA (siRNA) sequences directed against SOD2 (Silencer® Selects s13268 and s13269, Life Technologies, Carlsbad, CA; SOD2-1 and SOD2-2), ZEB1 s229970 and s229971, Life Technologies, Carlsbad, CA; ZEB1-1 and ZEB1-2), ZEB2 (s19032 and 19033, Life Technologies, Carlsbad, CA; ZEB2-1 and ZEB2-2), NF-κB p65 (Silencer® Selects s11915, Life Technologies, Carlsbad, CA;), or a non-silencing control sequence (Silencer Select Negative Control #1)(10 nM)(Life Technologies) were transfected transiently with Lipofectamine™ RNAi Max reagent (Life Technologies), following the manufacturer's instructions. Sixteen hours after the transfection, cells were exposed to hypoxia or normoxia, or treated with or without H_2O_2 for 48 h. Transient transfection of reporter plasmids and luciferase assays were performed as described previously [18]. Briefly, 200 ng of pSODLUC-3340 (a gift of Dr. Burgering, University Medical Center Utrecht), P7/pGL3 or I2E-P7/pGL3 [29-31] was transfected. Mean firefly luciferase activity was normalized

to co-transfected renilla luciferase activity. Transfection was carried out at least three times, and variation between experiments was less than 15%.

Real-time reverse-transcription polymerase chain reaction (RT-PCR)

RNA isolation, cDNA synthesis and real-time RT-PCR were performed using TaqMan® Gene Expression Assays (Applied Biosystems) for SOD2 (Hs00167309_m1), Catalase (Hs00156308_m1), GPX2 (Hs00702173_s1), GPX7 (Hs00210410_m1), *CDH1* (Hs00170423_m1), *CDH2* (Hs00983062_m1), *ZEB1* (Hs00232783_m1), *ZEB2* (Hs00207691_m1) as described [20]. SYBR green (Applied Biosystems) was used to quantitate mRNA for *β-actin* as described previously [18]. SYBR green was also used to quantitate mRNA for NF-κB p65, IL6 and IL8 with paired forward and reverse primers NF-κB p65-F (5′-CTCCGCGGGCAGCAT-3′) and NF-κB p65-R (5′-TCCTGTGTAGCCATTGATCTTGA T-3′); IL-6-F (5′-GCAGAAAAAGGCAAAGAATC-3′) and IL-6-R (5′-CTACATTTGCCGAAGAGC-3′); and IL-8-F (5′-CACCGGAAGGAACCATCTCA-3′) and IL-8-R (5′-TGGCAAAACTGCACCTT CACA-3′). Primer pairs specific to the 3′-UTR of the 1.5- and 4.2-kb *MnSOD* transcripts were used to determine their levels as described 28. Relative level of each mRNA was normalized to β-actin which serves as an internal control.

Western blotting

Whole cell lysates were prepared as described previously [18]. 20 μg of denatured protein was fractionated on a NuPAGE Bis-Tris 4–12% gel (Life Technologies). Following electrotransfer, Immobilon-P membranes (Millipore) were incubated with primary antibodies for NF-kB p65 (D14E12 XP® Rabbit mAb #8242, Cell Signaling Technology, Beverly, MA) at 1:1000, Phospho-NF-kB p65^{Ser536} (93H1 Rabbit mAb, #3033, Cell Signaling) at 1:1000, SOD2 (ab13534, Abcam, Cambridge, UK at 1:1000, GPX1 (#3206, Cell Signaling) at 1:1000 or Catalase (#8841, Cell Signaling) at 1:1000 and then with the appropriate HRP-conjugated secondary antibody (GE Healthcare, Piscataway, NJ). E-Cadherin, N-Cadherin, ZEB1, ZEB2 and β-actin (a loading control) were detected as described previously [20].

Immunofluorescence

Cells grown on glass coverslips precoated with bovine collagen (1μg/ml; Organogenesis, Canton MA) were fixed in 3% formaldehyde for 20 min, permeabilized with 0.1% Triton X-100 in PBS, and blocked with 5% bovine serum albumin for 1 hr. Cells were incubated with anti-SOD2 (1:100; ab13534, Abcam, Cambridge, UK) overnight at 4°C, and then with Rabbit-Cy2-conjugated secondary antibody (1: 600; Jackson ImmunoResearch, West Grove, PA) for 1 h at room temperature. Nuclei were counterstained by DAPI (1:10,000; Invitrogen). Stained objects were imaged with a Leica TCS SP8 confocal microscope using LAS software (Leica Microsystems, Buffalo Grove, IL).

Flow cytometry and Fluorescence Activated Cell Sorting (FACS)

Flow cytometry and FACS were performed as described previously [37]. To determine CD44^{high}-CD24$^{low/-}$ cells (CD44H) and CD44$^{low/-}$-CD24$^{low/-}$ cells (CD44L)

subpopulations, cells were suspended in Hank's balanced salt solution (Life Technologies) containing 1% BSA (Sigma-Aldrich) and stained with PE/Cy7-anti-CD24 at 1:10 (BioLegend, San Diego, CA) and APC-anti-CD44 at 1:20 (BD Biosciences) on ice for 30 min. FACS Vantage SE (BD Biosciences) was used to isolate CD44L and CD44H cells. Flow cytometry was repeated for each genotype and condition at least three times.

DCF assay

ROS were determined by flow cytometry with 2′, 7′-dichlorodihydrofluorescein diacetate (DCF) dye (Life Technologies) as described previously [37]. In brief, cells were incubated with 10 μM DCF at 37°C for 30 min and further cultured for up to 3 hours prior to flow cytometry. Cells were incubated with or without the antioxidant N-acetyl-L-cysteine (NAC) (Sigma-Aldrich, St. Louis, MO) at 10 mM or 1mM as indicated for 1 hour.

Statistical analyses

Data from experiments are presented as mean ± standard error (n=3) and were analyzed by two-tailed Student's *t* test. *P* <0.05 was considered significant.

Supplementary Material

Refer to Web version on PubMed Central for supplementary material.

Acknowledgments

References

1. Nieto MA. The ins and outs of the epithelial to mesenchymal transition in health and disease. Annu Rev Cell Dev Biol. 2011; 27:347–376. [PubMed: 21740232]

2. Kalluri R, Weinberg RA. The basics of epithelial-mesenchymal transition. J Clin Invest. 2009; 119:1420–1428. [PubMed: 19487818]

3. Thiery JP. Epithelial-mesenchymal transitions in tumour progression. Nature reviews Cancer. 2002; 2:442–454. [PubMed: 12189386]

4. De Craene B, Berx G. Regulatory networks defining EMT during cancer initiation and progression. Nature reviews Cancer. 2013; 13:97–110. [PubMed: 23344542]

5. Giannoni E, Parri M, Chiarugi P. EMT and oxidative stress: a bidirectional interplay affecting tumor malignancy. Antioxid Redox Signal. 2012; 16:1248–1263. [PubMed: 21929373]

6. Irani K, Xia Y, Zweier JL, Sollott SJ, Der CJ, Fearon ER, et al. Mitogenic signaling mediated by oxidants in Ras-transformed fibroblasts. Science. 1997; 275:1649–1652. [PubMed: 9054359]

7. Ansieau S, Bastid J, Doreau A, Morel AP, Bouchet BP, Thomas C, et al. Induction of EMT by twist proteins as a collateral effect of tumor-promoting inactivation of premature senescence. Cancer Cell. 2008; 14:79–89. [PubMed: 18598946]

8. Zoller M. CD44: can a cancer-initiating cell profit from an abundantly expressed molecule? Nature reviews Cancer. 2011; 11:254–267. [PubMed: 21390059]

9. Al-Hajj M, Wicha MS, Benito-Hernandez A, Morrison SJ, Clarke MF. Prospective identification of tumorigenic breast cancer cells. Proceedings of the National Academy of Sciences of the United States of America. 2003; 100:3983–3988. [PubMed: 12629218]

10. Prince ME, Sivanandan R, Kaczorowski A, Wolf GT, Kaplan MJ, Dalerba P, et al. Identification of a subpopulation of cells with cancer stem cell properties in head and neck squamous cell carcinoma. Proceedings of the National Academy of Sciences of the United States of America. 2007; 104:973–978. [PubMed: 17210912]

11. Mani SA, Guo W, Liao MJ, Eaton EN, Ayyanan A, Zhou AY, et al. The epithelial-mesenchymal transition generates cells with properties of stem cells. Cell. 2008; 133:704–715. [PubMed: 18485877]

12. Morel AP, Lievre M, Thomas C, Hinkal G, Ansieau S, Puisieux A. Generation of breast cancer stem cells through epithelial-mesenchymal transition. PLoS One. 2008; 3:e2888. [PubMed: 18682804]

13. Sena LA, Chandel NS. Physiological roles of mitochondrial reactive oxygen species. Molecular cell. 2012; 48:158–167. [PubMed: 23102266]

14. Thannickal VJ, Fanburg BL. Reactive oxygen species in cell signaling. Am J Physiol Lung Cell Mol Physiol. 2000; 279:L1005–1028. [PubMed: 11076791]

15. Lambert AJ, Brand MD. Reactive oxygen species production by mitochondria. Methods Mol Biol. 2009; 554:165–181. [PubMed: 19513674]

16. Radisky DC, Levy DD, Littlepage LE, Liu H, Nelson CM, Fata JE, et al. Rac1b and reactive oxygen species mediate MMP-3-induced EMT and genomic instability. Nature. 2005; 436:123–127. [PubMed: 16001073]

17. Zhou G, Dada LA, Wu M, Kelly A, Trejo H, Zhou Q, et al. Hypoxia-induced alveolar epithelial-mesenchymal transition requires mitochondrial ROS and hypoxia-inducible factor 1. Am J Physiol Lung Cell Mol Physiol. 2009; 297:L1120–1130. [PubMed: 19801454]

18. Kagawa S, Natsuizaka M, Whelan KA, Facompre N, Naganuma S, Ohashi S, et al. Cellular senescence checkpoint function determines differential Notch1-dependent oncogenic and tumor-suppressor activities. Oncogene. 2014; 0

19. Yoon YS, Lee JH, Hwang SC, Choi KS, Yoon G. TGF beta1 induces prolonged mitochondrial ROS generation through decreased complex IV activity with senescent arrest in Mv1Lu cells. Oncogene. 2005; 24:1895–1903. [PubMed: 15688038]

20. Ohashi S, Natsuizaka M, Wong GS, Michaylira CZ, Grugan KD, Stairs DB, et al. Epidermal growth factor receptor and mutant p53 expand an esophageal cellular subpopulation capable of epithelial-to-mesenchymal transition through ZEB transcription factors. Cancer Res. 2010; 70:4174–4184. [PubMed: 20424117]

21. Trachootham D, Lu W, Ogasawara MA, Nilsa RD, Huang P. Redox regulation of cell survival. Antioxid Redox Signal. 2008; 10:1343–1374. [PubMed: 18522489]

22. Zelko IN, Mariani TJ, Folz RJ. Superoxide dismutase multigene family: a comparison of the CuZn-SOD (SOD1), Mn-SOD (SOD2), and EC-SOD (SOD3) gene structures, evolution, and expression. Free Radic Biol Med. 2002; 33:337–349. [PubMed: 12126755]

23. Dhar SK, St Clair DK. Manganese superoxide dismutase regulation and cancer. Free Radic Biol Med. 2012; 52:2209–2222. [PubMed: 22561706]

24. Connor KM, Hempel N, Nelson KK, Dabiri G, Gamarra A, Belarmino J, et al. Manganese superoxide dismutase enhances the invasive and migratory activity of tumor cells. Cancer Research. 2007; 67:10260–10267. [PubMed: 17974967]

25. Huber MA, Azoitei N, Baumann B, Grunert S, Sommer A, Pehamberger H, et al. NF-kappaB is essential for epithelial-mesenchymal transition and metastasis in a model of breast cancer progression. The Journal of clinical investigation. 2004; 114:569–581. [PubMed: 15314694]

26. Thiery JP, Acloque H, Huang RY, Nieto MA. Epithelial-mesenchymal transitions in development and disease. Cell. 2009; 139:871–890. [PubMed: 19945376]

27. Lamouille S, Xu J, Derynck R. Molecular mechanisms of epithelial-mesenchymal transition. Nat Rev Mol Cell Biol. 2014; 15:178–196. [PubMed: 24556840]

28. Chaudhuri L, Nicholson AM, Kalen AL, Goswami PC. Preferential selection of MnSOD transcripts in proliferating normal and cancer cells. Oncogene. 2012; 31:1207–1216. [PubMed: 21804600]

29. Xu Y, Kiningham KK, Devalaraja MN, Yeh CC, Majima H, Kasarskis EJ, et al. An intronic NF-kappaB element is essential for induction of the human manganese superoxide dismutase gene by tumor necrosis factor-alpha and interleukin-1beta. DNA Cell Biol. 1999; 18:709–722. [PubMed: 10492402]

30. Kim HP, Roe JH, Chock PB, Yim MB. Transcriptional activation of the human manganese superoxide dismutase gene mediated by tetradecanoylphorbol acetate. The Journal of biological chemistry. 1999; 274:37455–37460. [PubMed: 10601319]

31. Yeh CC, Wan XS, St Clair DK. Transcriptional regulation of the 5′ proximal promoter of the human manganese superoxide dismutase gene. DNA Cell Biol. 1998; 17:921–930. [PubMed: 9839801]

32. Ohashi S, Natsuizaka M, Naganuma S, Kagawa S, Kimura S, Itoh H, et al. A NOTCH3-mediated squamous cell differentiation program limits expansion of EMT-competent cells that express the ZEB transcription factors. Cancer Research. 2011; 71:6836–6847. [PubMed: 21890822]

33. Ovcharenko I, Nobrega MA, Loots GG, Stubbs L. ECR Browser: a tool for visualizing and accessing data from comparisons of multiple vertebrate genomes. Nucleic Acids Res. 2004; 32:W280–286. [PubMed: 15215395]

34. Rhyu DY, Yang Y, Ha H, Lee GT, Song JS, Uh ST, et al. Role of reactive oxygen species in TGF-beta1-induced mitogen-activated protein kinase activation and epithelial-mesenchymal transition in renal tubular epithelial cells. J Am Soc Nephrol. 2005; 16:667–675. [PubMed: 15677311]

35. Lin CH, Hung PH, Chen YJ. CD44 Is Associated with the Aggressive Phenotype of Nasopharyngeal Carcinoma through Redox Regulation. Int J Mol Sci. 2013; 14:13266–13281. [PubMed: 23803658]

36. Gammon L, Biddle A, Heywood HK, Johannessen AC, Mackenzie IC. Sub-sets of cancer stem cells differ intrinsically in their patterns of oxygen metabolism. PLoS One. 2013; 8:e62493. [PubMed: 23638097]

37. Natsuizaka M, Kinugasa H, Kagawa S, Whelan KA, Naganuma S, Subramanian H, et al. IGFBP3 promotes esophageal cancer growth by suppressing oxidative stress in hypoxic tumor microenvironment. Am J Cancer Res. 2014; 4:29–41. [PubMed: 24482736]

38. Ishimoto T, Nagano O, Yae T, Tamada M, Motohara T, Oshima H, et al. CD44 variant regulates redox status in cancer cells by stabilizing the xCT subunit of system xc(-) and thereby promotes tumor growth. Cancer Cell. 2011; 19:387–400. [PubMed: 21397861]

39. Dhar SK, Tangpong J, Chaiswing L, Oberley TD, St Clair DK. Manganese superoxide dismutase is a p53-regulated gene that switches cancers between early and advanced stages. Cancer Research. 2011; 71:6684–6695. [PubMed: 22009531]

40. Guha M, Srinivasan S, Ruthel G, Kashina AK, Carstens RP, Mendoza A, et al. Mitochondrial retrograde signaling induces epithelial-mesenchymal transition and generates breast cancer stem cells. Oncogene. 2013

41. Chua HL, Bhat-Nakshatri P, Clare SE, Morimiya A, Badve S, Nakshatri H. NF-kappaB represses E-cadherin expression and enhances epithelial to mesenchymal transition of mammary epithelial cells: potential involvement of ZEB-1 and ZEB-2. Oncogene. 2007; 26:711–724. [PubMed: 16862183]

42. Nam EH, Lee Y, Zhao XF, Park YK, Lee JW, Kim S. ZEB2-Sp1 cooperation induces invasion by upregulating cadherin-11 and integrin alpha5 expression. Carcinogenesis. 2014; 35:302–314. [PubMed: 24130169]

43. Nam EH, Lee Y, Park YK, Lee JW, Kim S. ZEB2 upregulates integrin alpha5 expression through cooperation with Sp1 to induce invasion during epithelial-mesenchymal transition of human cancer cells. Carcinogenesis. 2012; 33:563–571. [PubMed: 22227038]

44. Chen PM, Wu TC, Wang YC, Cheng YW, Sheu GT, Chen CY, et al. Activation of NF-kappaB by SOD2 promotes the aggressiveness of lung adenocarcinoma by modulating NKX2-1-mediated IKKbeta expression. Carcinogenesis. 2013; 34:2655–2663. [PubMed: 23784082]

45. Meng X, Wu J, Pan C, Wang H, Ying X, Zhou Y, et al. Genetic and epigenetic down-regulation of microRNA-212 promotes colorectal tumor metastasis via dysregulation of MnSOD. Gastroenterology. 2013; 145:426–436. e421–426. [PubMed: 23583431]

46. Ji G, Lv K, Chen H, Wang T, Wang Y, Zhao D, et al. MiR-146a regulates SOD2 expression in H2O2 stimulated PC12 cells. PLoS One. 2013; 8:e69351. [PubMed: 23935993]

47. Bai XY, Ma Y, Ding R, Fu B, Shi S, Chen XM. miR-335 and miR-34a Promote renal senescence by suppressing mitochondrial antioxidative enzymes. J Am Soc Nephrol. 2011; 22:1252–1261. [PubMed: 21719785]

48. Kriegel AJ, Fang Y, Liu Y, Tian Z, Mladinov D, Matus IR, et al. MicroRNA-target pairs in human renal epithelial cells treated with transforming growth factor beta 1: a novel role of miR-382. Nucleic acids research. 2010; 38:8338–8347. [PubMed: 20716515]

49. Liu X, Yu J, Jiang L, Wang A, Shi F, Ye H, et al. MicroRNA-222 regulates cell invasion by targeting matrix metalloproteinase 1 (MMP1) and manganese superoxide dismutase 2 (SOD2) in tongue squamous cell carcinoma cell lines. Cancer Genomics Proteomics. 2009; 6:131–139. [PubMed: 19487542]

50. Wang Q, Wang Y, Minto AW, Wang J, Shi Q, Li X, et al. MicroRNA-377 is up-regulated and can lead to increased fibronectin production in diabetic nephropathy. FASEB journal : official publication of the Federation of American Societies for Experimental Biology. 2008; 22:4126–4135. [PubMed: 18716028]

51. Ju X, Casimiro MC, Gormley M, Meng H, Jiao X, Katiyar S, et al. Identification of a cyclin D1 network in prostate cancer that antagonizes epithelial-mesenchymal restraint. Cancer Research. 2014; 74:508–519. [PubMed: 24282282]

52. Dickson MA, Hahn WC, Ino Y, Ronfard V, Wu JY, Weinberg RA, et al. Human keratinocytes that express hTERT and also bypass a p16(INK4a)-enforced mechanism that limits life span become immortal yet retain normal growth and differentiation characteristics. Molecular and cellular biology. 2000; 20:1436–1447. [PubMed: 10648628]

Abbreviations

|	
EMT	epithelial-mesenchymal transition
FACS	fluorescence activated cell sorting
MnSOD	manganese superoxide dismutase
NAC	N-acetyl-L-cysteine
RNAi	RNA interference
ROS	reactive oxygen species
RT-PCR	reverse-transcription polymerase chain reaction
SABG	senescence-associated β-galactosidase activity
siRNA	small interfering RNA
SOD2	superoxide dismutase 2
TGF-β	transforming growth factor-β
NAC	N-acetylcysteine
CSC	cancer stem cell
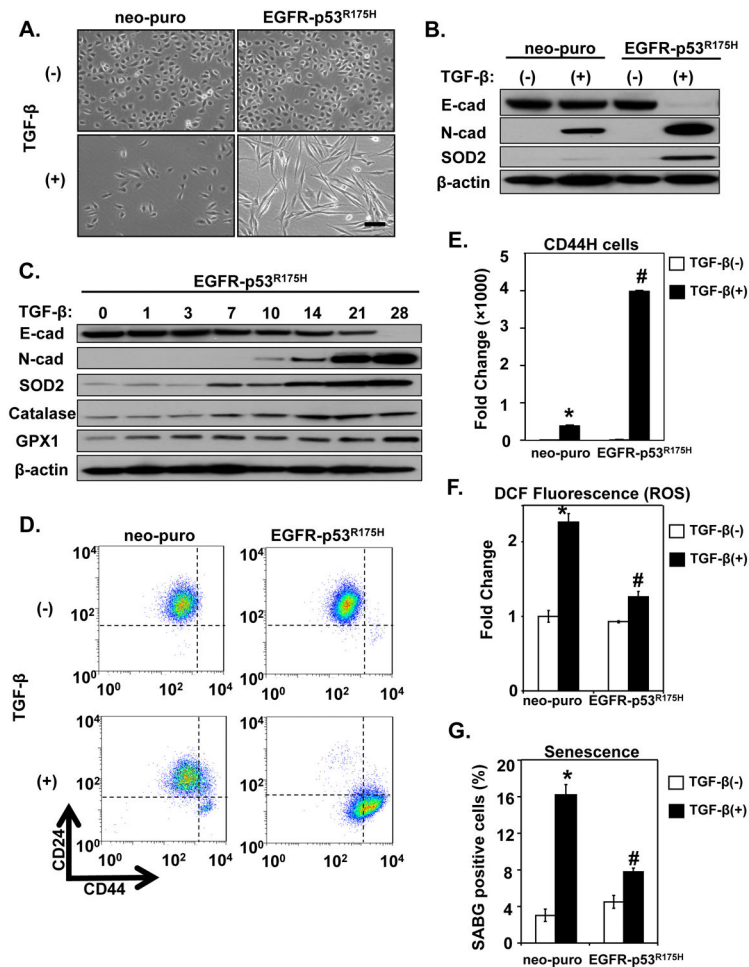
Figure 1. Differential responses of transformed and non-transformed esophageal keratinocytes to TGF-β

EPC2-hTERT-EGFR-p53^{R175H} (transformed) or neo-puro control (non-transformed) cells were stimulated with TGF-β (5 ng/ml). After 28 days, representative phase contrast images were taken in (**A**) and cells were assessed for expression of indicated proteins by immunoblot analysis with β-actin serving as a loading control in (**B**). Following treatment for indicated time periods, EGFR-p53^{R175H} cells were subjected to immunoblot analysis in (**C**). β-actin was used as a loading control. After 28 days, EGFR-p53^{R175H} and neo-puro cells were analyzed for expression of CD24 and CD44 by flow cytometry in (**D**). Note CD44H cells are present in the lower right quadrant. Fold change in CD44H cells was determined in (**E**). Induction of ROS was determined flow cytometric analysis for DCF stained cells in (**F**). Senescence was assessed by SABG staining in (**G**). *, $p<0.05$ vs. neo-puro TGF-β(-); #, $p<0.05$ vs. neo-puro TGF-β(+); (n=3) in (**E-G**).
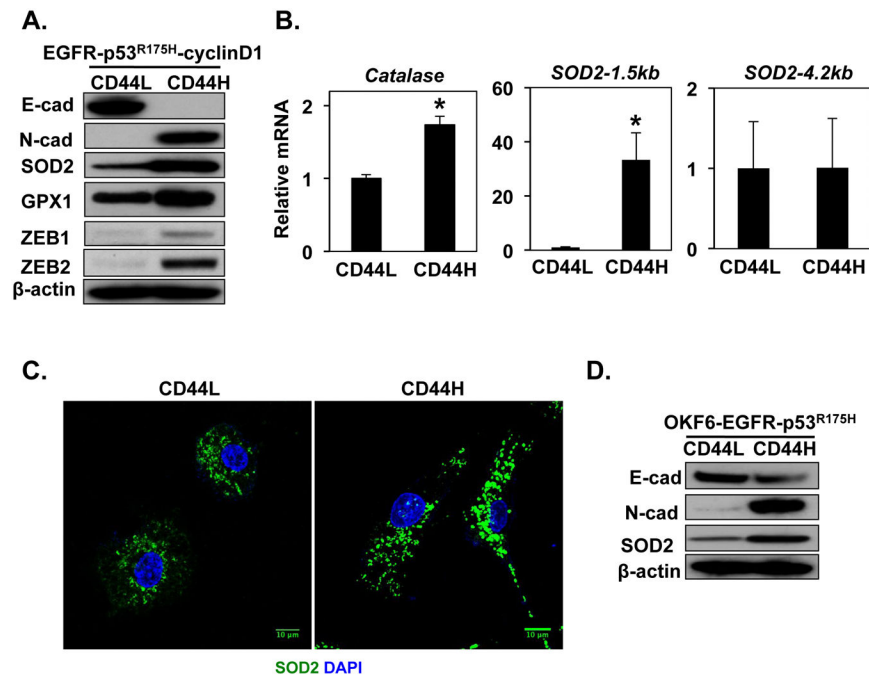
A.

EGFR-p53^R175H^-cyclinD1

	CD44L	CD44H
E-cad		
N-cad		
SOD2		
GPX1		
ZEB1		
ZEB2		
β-actin		

B.

Catalase

SOD2-1.5kb

SOD2-4.2kb

C.

CD44L   CD44H

SOD2 DAPI

D.

OKF6-EGFR-p53^R175H^

	CD44L	CD44H
E-cad		
N-cad		
SOD2		
β-actin		

Figure 2. SOD2 is induced during TGF-β-mediated EMT

CD44L and CD44H subpopulations were isolated from EPC2T and OKF6-Tert2-EGFR-p53^R175H^ cells by FACS. (**A**) CD44L and CD44H cells from EPC2T were assessed for protein expression by immunoblot analysis. β-actin was used as a loading control. (**B**) qRT-PCR analysis was used to examine expression of catalase as well as SOD2-1.5kb and -4.2kband transcript variants in EPC2T CD44L and CD44H cells. (**C**) Expression of SOD2 (green) was assessed in EPC2T CD44L and CD44H cells by immunofluorescence. DAPI (blue) was used to visualize nuclei. (**D**) CD44L and CD44H cells from OKF6-hTERT-EGFR-p53^R175H^ were assessed for protein expression by immunoblot analysis. β-actin was used as a loading control. *, $p<0.05$ vs. CD44L (n=3).
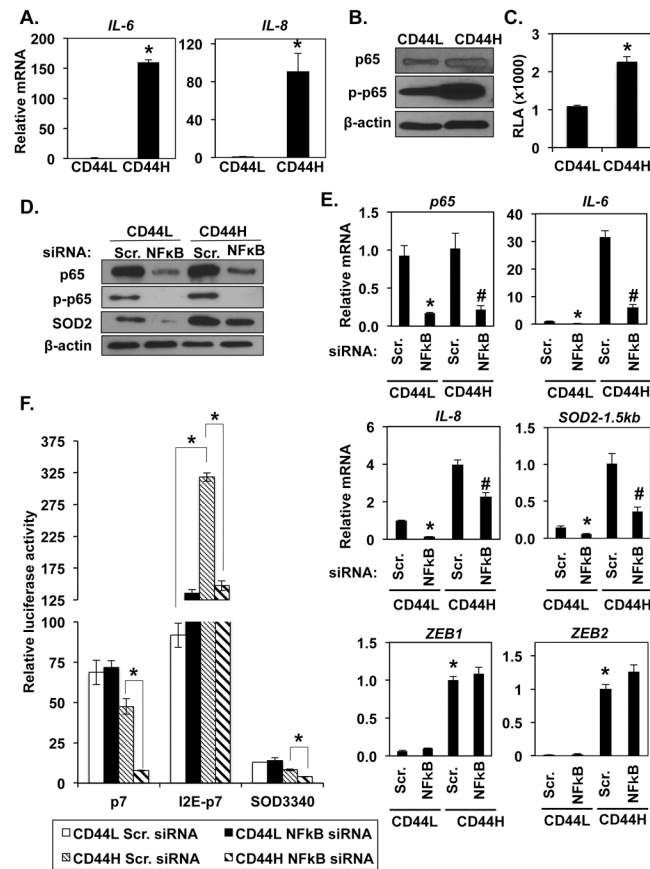
Figure 3. SOD2 expression during EMT is regulated by NF-kB

CD44L and CD44H subpopulations were isolated from EPC2T cells by FACS. (**A**) qRT-PCR analysis was used to examine expression of indicated genes. *, $p<0.05$ vs. CD44L (n=3). (**B**) Expression of indicated proteins was evaluated by immunoblot analysis. β-actin served as a loading control. p-p65, phospho-NF-kB p65[Ser536]. (**C**) Cells transfected with a pGL3- NF-κB reporter construct or empty pGL3 vector were assessed for luciferase activity. *, $p<0.05$ vs. CD44L; (n=3). (**D and E**) Cells transfected with siRNA targeting NF-κB or a scramble control sequence (Scr.) were subjected to immunoblot (**D**) or qRT-PCR (**E**) analyses. β-actin was used as a loading control in (**D**) and as an internal control in (**E**) and *, $p<0.05$ vs. CD44L and Scr.; #, $p<0.05$ vs. CD44H and Scr. (n=3). (**F**) Cells transfected with siRNA targeting NF-κB or a scramble control (Scr.) sequence were then transfected with indicated SOD2 promoter reporter constructs or empty pGL3 to evaluate luciferase activity. *, $p<0.05$;. (n=3).
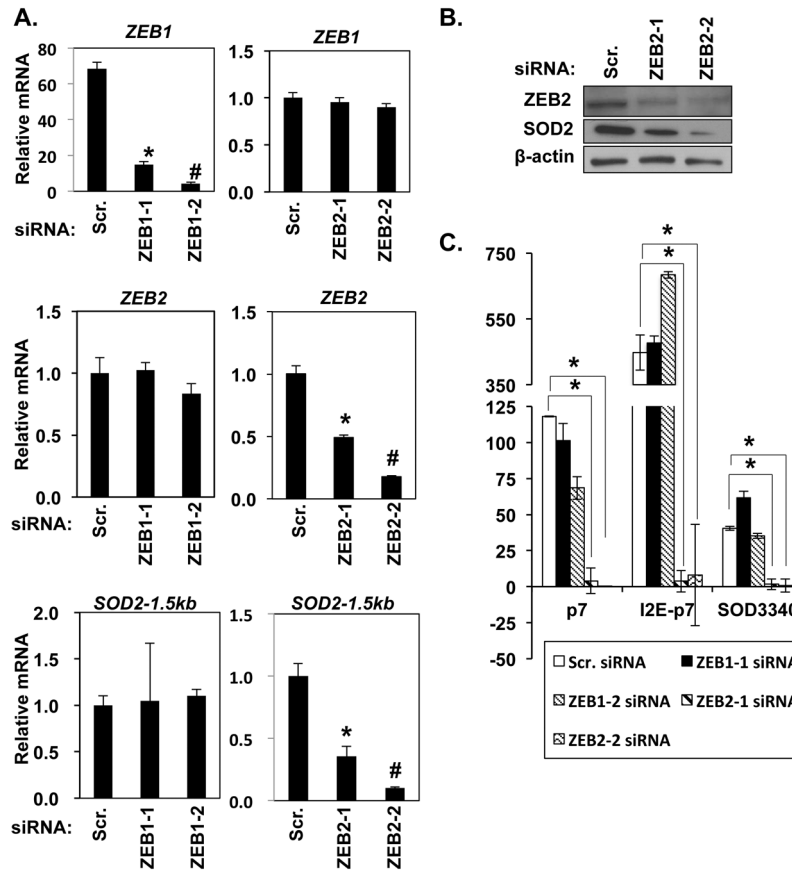
Figure 4. ZEB2, but not ZEB1, modulates SOD2 induction during EMT
CD44L and CD44H subpopulations were isolated from EPC2T cells by FACS. (**A-C**) Cells were transfected with siRNA targeting ZEB1, ZEB2 or a scramble control (Scr.) sequence for qRT-PCR (**A**) and immunoblot (**B**) analyses. β-actin was used as an internal control in (**A**) and a loading control in (**B**). In (**C**), cells were further transfected with indicated SOD2 promoter reporter constructs or empty pGL3 to evaluate luciferase activity. *, $p<0.05$; (n=3).
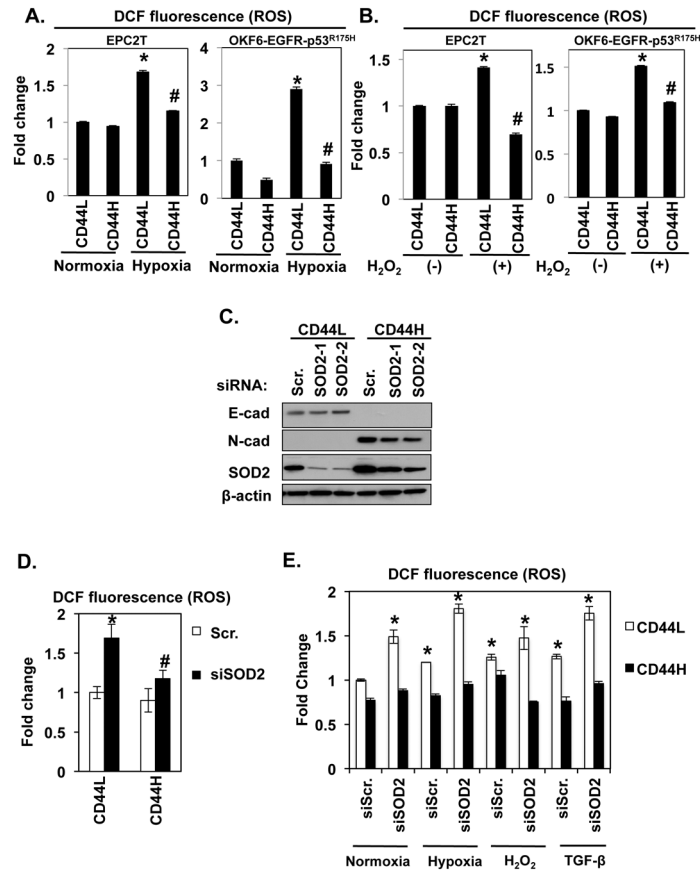
Figure 5. Differential SOD2 expression in CD44L and CD44H cells influences ROS induction in response to oxidative stress-inducing stimuli
CD44L and CD44H subpopulations isolated from EPC2T and OKF6-Tert2-EGFR-p53^{R175H} cells by FACS. (**A**) Cells were cultured in normoxic (21% O_2) or hypoxic (0.5% O_2) conditions for 48 hrs and analyzed by flow cytometry. *, $p<0.05$ vs. CD44L and normoxia; #, $p<0.05$ vs. CD44L and hypoxia; (n=3). (**B**) Cells were cultured in the presence or absence of H_2O_2 (200 μM) for 24 hrs then stained with DCF and analyzed by flow cytometry. *, $p<0.05$ vs. CD44L and H_2O_2 (-); #, $p<0.05$ vs. CD44L and H_2O_2 (+); (n=3). EPC2T CD44L and CD44H cells were transfected with siRNA targeting SOD2 or a scramble control sequence then assessed for expression of indicated proteins by immunoblot (**C**) or subjected to flow cytometric analysis of DCF fluorescence (**D** and **E**). *, $p<0.05$ vs. Scr.; (n=3).
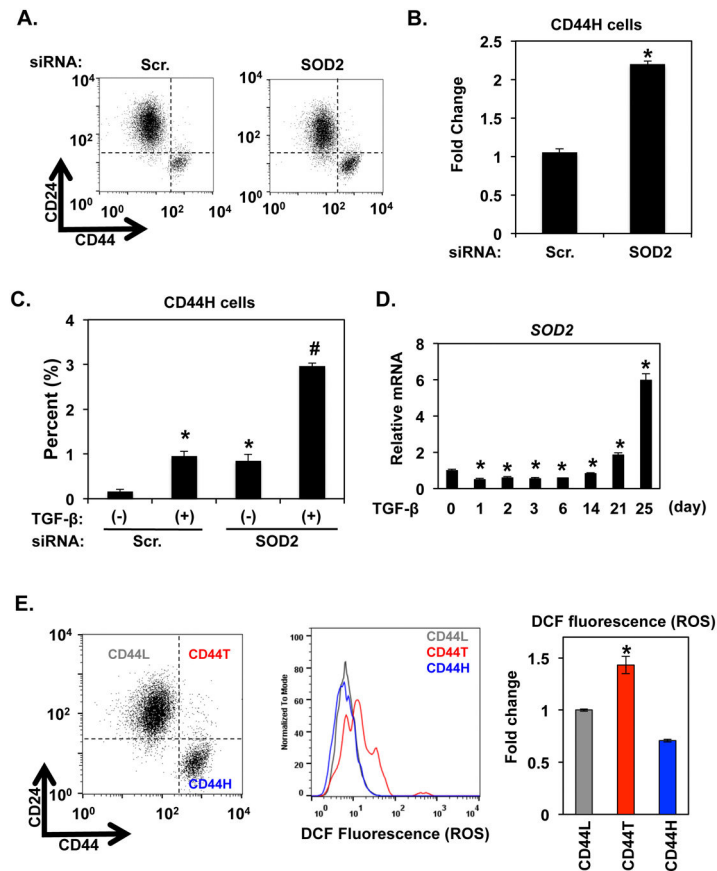
Figure 6. SOD2 expression may limit EMT by suppressing ROS in CD44L cells

(**A**) EPC2T cells were transfected with siRNA targeting SOD2 or a scramble control sequence. Four days following transfection, cells were assessed by flow cytometry for distribution of CD24 and CD44 and fold change in CD44H cells (lower right quadrant) was quantified in (**B**). *, $p<0.05$ vs. si-Scramble TGF-β (-); #, $p<0.05$ vs. si-SOD2 and TGF-β (-); (n=3). (**C**) CD44L cells purified from EPC2T cells were transfected with siRNA targeting SOD2 or a scramble control sequence. After 4 days of treatment with TGF-β, expression of CD24 and CD44 was assessed by flow cytometry and induction of CD44H cells was quantified. (**D**) EPC2T CD44L cells stimulated with TGF-β for indicated time points were assessed for expression of SOD2 RNA by qRT-PCR. *, $p<0.05$ vs. TGF-β at day 0; (n=3). (**E**). EPC2T cells were stained then analyzed for DCF and expression of CD24 and CD44 by flow cytometry. Subpopulations were gated as indicated and the relative DCF fluorescence was determined. *, $p<0.05$ vs. CD44L; (n=3).